IEEE Transactions on Energy Conversion, Vol. 7, No. 3, September 1992.

Control of a Linear Permanent Magnet Brushless Dc Motor Via Exact Linearization Methods

Parviz Famouri
Department of Electrical & Computer Engineering
West Virginia University
Morgantown, WV 26506-6101

ABSTRACT

This paper presents a nonlinear feedback control design methodology for a linear motion, permanent magnet brushless dc motor. A nonlinear state variable model for the motor, including the cogging force, is derived. Computer simulations of the resulting closed-loop system are given to demonstrate the effectiveness of the proposed control laws. Finally, simulation results of the control variables are injected into the actual nonlinear system in an experimental open-loop setup to validate the design procedure. Although here the control objective is a brushless dc servo motor with linear action, the methodology developed is equally applicable to rotary permanent magnet brushless dc motors.

Keywords: Permanent Magnet Brushless DC Motor, Nonlinear Control, Exact Linearization

Nomenclature

x_p	translational position
x_{1d}	desired translational position
$\dot{x}_p$	translator speed
x_{2d}	desired translational speed
i_q	quadrature-axis current
x_{3d}	desired quadrature-axis current
i_d	direct-axis current
x_{4d}	desired direct-axis current
M	translator mass
β	damping coefficient
τ	pole pitch
L_q	quadrature-axis inductance
L_d	direct-axis inductance
L_{ls}	phase leakage inductance
λ_{max}	maximum value of the fundamental component of flux linkages due to the PM field
r	per phase resistance
F_{ri}	maximum value of the i th component of cogging force
F_L	load force
v_q	quadrature-axis voltage
v_d	direct-axis voltage

1. Introduction

Permanent magnet brushless dc motors (PMBDCM) are a relatively recent development in motor technology when compared to conventional dc (shunt, series) or ac (induction, synchronous) motors. Appreciation of PMBDCMs was limited by the unavailability of high power semiconductor drivers that are needed for these motors. However, with recent advances in power semiconductor technology, interest in PMBDCMs has grown over the last few years [1]-[4]. More design engineers are selecting PMBDCMs over conventional dc or induction motor drives for the following reasons: 1) The absence of the brushes results in essentially a maintenance free operation, and eliminates the undesirable effects of commutation such as sparks (which is hazardous in flammable environments), brush loss, radio-frequency interference, etc. 2) The low inertia of the rotor increases the mechanical response of the motor, shortening the acceleration and deceleration time. 3) Utilizing rare-earth permanent magnet materials with high coercive force results in substantially higher power to weight ratios as compared to a conventional dc motor of the same size, hence, PMBDCMs operate at 20 to 50 percent higher efficiency than their brush counterpart of the same size [1]. 4) In despite of conventional dc motors where the armature windings are located in the rotor, the armature windings of PMBDCMs are located in the stator. Thus, placing heat sinks on the outside of stator frame results in a lower temperature in the armature windings, thereby expanding current density operation range. 5) Because of the absence of commutator segments, the rotor construction is simple.

92 WM 300-4 EC A paper recommended and approved by the IEEE Electric Machinery Committee of the IEEE Power Engineering Society for presentation at the IEEE/PES 1992 Winter Meeting, New York, New York, January 26-30, 1992. Manuscript submitted September 3, 1991; made available for printing January 9, 1992.

Since the system equations are highly nonlinear, a systematic method of solution for the optimized control regime has not yet been developed. While there are number of frequency and time domain techniques for designing controllers for linear systems, similar methods do not exist for nonlinear systems. One method used to develop a controller for nonlinear systems is to obtain a linearized model of the system about the states operating point. This model is only valid for small perturbations. By applying linear control theory, a controller is designed for every operating point. Because of the wide range of operating conditions and approximate nature of the linearized system, this type of a controller does not meet the high dynamical performance requirement for servo applications. However, with today's rapid growth in microelectronics technology and development of fast digital signal processing chips, more complex control laws can be implemented in real time. Before we proceed, a review of recent literature on the PMBDCM is appropriate.

A vast body of literature is available on analysis of the PMBDCMs [1]-[3], however, we will concentrate on publications related to the control [4]-[8]. Meshkat and Persson [4] have presented a regime for controlling the phase currents such that the direct axis current i_d remains at zero. Le-Huy, et al. [5] described current control to obtain a current which interacts with the back emf in such a manner as to produce constant power. This constant power in turn produces a constant torque at a constant speed. Both of these methods are valid only when the PMBDCM has reached steady-state and do not address the problem of controlling the transient response of the motor. Hashimoto et al. [6] and El-Sharkawi [7] controlled a PMBDCM by a Variable Structure System (VSS). Although VSS control is an effective control strategy for nonlinear systems such as the PMBDCM, theoretical results are valid only while the system is in the sliding mode and the control which drives the system into the sliding condition is discontinuous. Discontinuous controls not only heighten the difficulty of the analysis of the closed-loop system model, but also, causes problems such as chattering in the physical system as well.

Hemati et al. [8] has developed a nonlinear controller for brushless dc motors, however, they failed to consider the reluctance (cogging) effects of the motor. This effect is extremely important for servo applications and is pronounced at low speed operations. They also have concentrated on the implementation through computer simulation and no experimental verification of the controller is presented. Their feedback loop contains derivative terms which in practical implementation will introduce noise and may cause overall system instability.

The purpose of this paper is to develop a position controller for PMBDCMs which systematically determines control laws for operation in both transient and steady-state with consideration of reluctance force. The controller design is based on a differential

geometric approach which assists the motor in overcoming its inherent deficiencies such as effects of torque ripples and reluctance torque. This will be achieved by transforming the nonlinear state equations into an exact linear model.

Recently, much interest has focused upon the problem of linearization of nonlinear systems [8]-[14]. The objective is to transform a nonlinear system into an equivalent linear representation in which linear control design can be performed. The following is a brief description of the major results in this area.

In 1978, Brockett [10] showed that by application of a nonlinear coordinate transformation and state feedback, a single input nonlinear system can be shown to be equivalent to a controllable linear system. Jakubczky and Respondek [11] extended Brockett's work and found necessary and sufficient conditions for the existence of a nonlinear coordinate transformation which relates a multi-input nonlinear system to an equivalent controllable linear system. Su [12] developed conditions which are more general than Brockett's for transforming a single-input nonlinear system into a controllable linear system. Finally, Hunt, Su, Meyer [13] generalized Su's work to multi-input nonlinear systems. This exact linearization method transforms the nonlinear model of the LPMBDCM to a linear controllable space thereby availing the abundance of tools of linear modern control theory to the designer.

2. Nonlinear State Variable Model

A permanent magnet synchronous motor is combined with a power conditioning unit and a position sensor to form a brushless dc motor. These motors can have rotary or linear motion. Although a brushless dc motor operates with ac currents flowing in its windings, the addition of a power conditioner produces behavior in a brushless dc motor similar to the behavior of a shunt dc motor in that the speed and torque are controlled by the magnitude of the applied voltage. We have built a prototype three phase, linear permanent magnet brushless dc motor (LPMBDCM). The LPMBDCM, shown in cross sectional view in Figure 1, is a linear motor with principle of operation similar to that of a rotary PMBDCM. The tube-shaped stator of the LPMBDCM can be conceptually produced by longitudinally cutting and flattening the rotary machine, and then rerolling the stator in the opposite direction. The secondary, known as the translator, is composed of permanent magnets in tandem on a moving cylinder and supported by linear motion bearings. The static force was measured for the rated current, and magnetic linearity was observed. The experimentally measured parameters of the motor under study are given in Appendix A. Industrial applications for LPMBDCMs can include displacement pumps, variable stroke solenoids, and direct drive prismatic actuator for robot manipulators. For the sake of brevity, we include the derivation of the state variable model for our LPMBDCM in Appendix B.

The state variable model for our LPMBDCM is given by

$$\frac{dx_p}{dt} = \dot{x}_p \tag{1}$$

$$\frac{d\dot{x}_p}{dt} = \frac{-\beta}{M}\dot{x}_p + \frac{\pi}{M\tau}(L_d - L_q)\, i_q i_d + \sqrt{\frac{3}{2}}\frac{\pi}{M\tau}\lambda_{max}\, i_q - \frac{F_L}{M} - \sum_{i=1}^{4}\frac{F_{ri}}{M}\sin\frac{6\pi i(x_p)}{\tau} \tag{2}$$

$$\frac{di_q}{dt} = \frac{-r}{L_q} i_q - \frac{\pi}{\tau}\frac{L_d}{L_q}\dot{x}_p i_d - \sqrt{\frac{3}{2}}\frac{\pi}{\tau}\frac{\lambda_{max}}{L_q}\dot{x}_p + \frac{v_q}{L_q} \tag{3}$$

$$\frac{di_d}{dt} = \frac{-r}{L_d} i_d + \frac{\pi}{\tau}\frac{L_q}{L_d}\dot{x}_p i_q + \frac{v_d}{L_d} \tag{4}$$

The last term of the right hand side of (2) is the model of the reluctance force. Reluctance force is produced by interaction between the permanent magnet fields and lamination materials. Thus, under no excitation this force still exists as a periodic force with six cycles per pole pitch. The effects of reluctance force is more apparent at low speeds, since at high speeds the reluctance force is small relative to the developed force of the motor. The reluctance force was first measured and analyzed via a discrete Fourier transform and the first four harmonics were chosen to describe the force.

One of the conditions for applicability of transformation of the

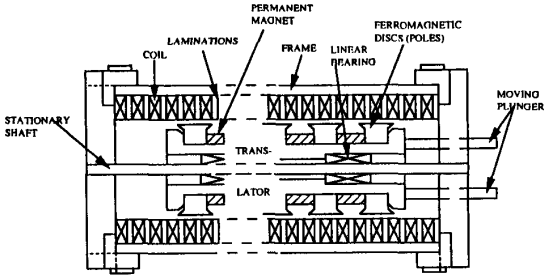

Figure 1: Cross sectional view of a LPMBDCM

nonlinear system to linear system is that the nonlinear system must be at equilibrium when all the states are at the origin. Therefore, a change of coordinates is necessary. The problem of position, speed, or current control becomes one of regulating error in the state variables to the origin. These state variable deviations are defined by

$$x_1 = x_p - x_{1d} \tag{5}$$

$$x_2 = \dot{x}_p - x_{2d} \tag{6}$$

$$x_3 = i_q - x_{3d} \tag{7}$$

$$x_4 = i_d - x_{4d}. \tag{8}$$

Since we are interested in position control, the desired speed must be zero, and for maximum output force per ampere, the desired d-axis current should also be zero [2], or

$$x_{2d} = x_{4d} = 0.$$

For the sake of simplified notation, we will set

$$k_1 = \frac{\pi}{M\tau}(L_d - L_q);\ k_2 = \sqrt{\frac{3}{2}}\frac{\pi}{M\tau}\lambda_{max};\ k_3 = \frac{-\beta}{M};\ k_4 = \frac{-r}{L_q};$$

$$k_5 = \frac{-\pi}{\tau}\frac{L_d}{L_q};\quad k_6 = \sqrt{\frac{3}{2}}\frac{\pi}{\tau}\frac{\lambda_{max}}{L_q};\ k_7 = \frac{-r}{L_d};\ k_8 = +\frac{\pi}{\tau}\frac{L_q}{L_d};$$

$$k_{9i} = \frac{-F_{ri}}{M};\ k_{10} = \frac{-F_L}{M};\ \omega_i = \frac{6\pi i(x_1 + x_{1d})}{\tau};$$

$$u_1 = k_4 x_{3d} + \frac{v_q}{L_q};\ u_2 = \frac{v_d}{L_d}.$$

Solving (5)-(8) for x_p, $\dot{x}_p$, i_q, and i_d and substituting into (1) - (4) yields the new nonlinear state equations for LPMBDCM in the new coordinates in the following form

$$\dot{x}(t) = f(x(t)) + \sum_{i=1}^{2} u_i(t) g_i \tag{9}$$

where

$$f(x(t)) = \begin{bmatrix} x_2 \\ k_3 x_2 + k_1 x_3 x_4 + k_2(x_3 + x_{3d}) + k_1 x_{3d} x_4 + \sum_{i=1}^{4} k_{9i}\sin\omega_i + k_{10} \\ k_4 x_3 + k_5 x_2 x_4 + k_6 x_2 \\ k_7 x_4 + k_8 x_2 x_3 + k_8 x_2 x_{3d} \end{bmatrix};$$

and

$$g_1 = \begin{bmatrix} 0 \\ 0 \\ 1 \\ 0 \end{bmatrix};\ g_2 = \begin{bmatrix} 0 \\ 0 \\ 0 \\ 1 \end{bmatrix}$$

are vector fields which are C^{∞} in an open set U in $\mathbb{R}^4$ containing origin, $f(0)=0$ and $u(t)$ is given by

$$u(t) = \begin{bmatrix} u_1 \\ u_2 \end{bmatrix} = \begin{bmatrix} k_4 x_{3d} + \frac{V_q}{L_q} \\ \frac{V_d}{L_d} \end{bmatrix}.$$

Since the state variable $x_1(t)$ represents the translational position error, the problem of position control of the motor is equivalent to regulating the states of (9) to the origin. Further, with x_{1d} known, x_{3d} can be found from the solution of (9) in steady state form to yield

$$x_{3d} = \sum_{i=1}^{4} \frac{-k_{9i}}{k_2} \sin\left(\frac{6\pi i x_{1d}}{\tau}\right) + \frac{k_{10}}{k_2} \qquad (10)$$

Therefore, upon setting a desired value for position, (10) specifies a desired value for q-axis current. Equation (9) is a set of nonlinear simultaneous differential equations, where $u(t)$ serve as the control inputs.

3. Modeling the LPMBDCM Via Exact Linearization

The necessary and sufficient conditions for the existence of a transformation to transform a nonlinear system to a linear system are known [13]. Applicability was investigated for our LPMBDCM and conditions have been verified in Appendix C. The procedure of [13] has been applied to the LPMBDCM (see Appendix C), and we have constructed a transformation which will bring (9) into an equivalent linear controllable model in Brunovsky canonical form

$$\dot{y} = \hat{A} y + \hat{B} v \qquad (11)$$

where

$$\hat{A} = \begin{bmatrix} 0 & 1 & 0 & 0 \\ 0 & 0 & 1 & 0 \\ 0 & 0 & 0 & 0 \\ 0 & 0 & 0 & 0 \end{bmatrix}, \quad \hat{B} = \begin{bmatrix} 0 & 0 \\ 0 & 0 \\ 1 & 0 \\ 0 & 1 \end{bmatrix},$$

or in the expanded form

$$\dot{y}_1 = y_2 \qquad (12)$$

$$\dot{y}_2 = y_3 \qquad (13)$$

$$\dot{y}_3 = v_1 \qquad (14)$$

$$\dot{y}_4 = v_2 \qquad (15)$$

where y_1, y_2, y_3, and y_4 are states in linear space and v_1 and v_2 are the new control variables. The state variables in linear space are related to state variable in nonlinear space as follows

$$y_1 = \frac{x_1}{k_2} \qquad (16)$$

$$y_2 = \frac{x_2}{k_2} \qquad (17)$$

$$y_3 = \frac{k_3}{k_2} x_2 + \left(\frac{k_1}{k_2} x_4 + 1\right)(x_3 + x_{3d}) + \sum_{i=1}^{4} \frac{k_{9i}}{k_2} \sin\omega_i + \frac{k_{10}}{k_2} \qquad (18)$$

$$y_4 = x_4 + \left[\sum_{i=1}^{4} k_{9i} \sin\omega_i + k_{10}\right] \frac{k_8}{k_2} x_1 \qquad (19)$$

and the new control variables in nonlinear space are related to the control variables in linear space as follows

$$\begin{bmatrix} v_1 \\ v_2 \end{bmatrix} = \begin{bmatrix} 1 + \frac{k_1}{k_2} x_4 & \frac{k_1}{k_2}(x_3 + x_{3d}) \\ 0 & 1 \end{bmatrix} \begin{bmatrix} u_1 \\ u_2 \end{bmatrix} + \begin{bmatrix} D(x) \\ E(x) \end{bmatrix} \qquad (20)$$

where $D(x)$ and $E(x)$ are defined in Appendix C. Note that by substituting (16) - (20) into (12) - (15), the original nonlinear system equations can be derived. This shows the validity of the transformation. Since the 2x2 matrix of (20) is invertible, therefore, we can solve for u

$$\begin{bmatrix} u_1 \\ u_2 \end{bmatrix} = \begin{bmatrix} (1 + \frac{k_1}{k_2} x_4)^{-1} & \frac{-k_1(x_3 + x_{3d})}{k_2 + k_1 x_4} \\ 0 & 1 \end{bmatrix} + \begin{bmatrix} v_1 - D(x) \\ v_2 - E(x) \end{bmatrix} \qquad (21)$$

We have now transformed our original nonlinear system model (9) into a linear equivalent model of (11). From this point on, we have an abundance of options available to us to design a feedback controller for (11) which regulates the states to the origin. Since (11) is related to the original system via transformation, we know that the origin of (11) maps into the origin of (9). Therefore, by regulating (11) to the origin we have succeeded in solving the original, nonlinear position control problem of the LPMBDCM.

4. Feedback Controller Design

Since (11) is controllable, we could use a variety of linear feedback design techniques to achieve regulation to the origin. Techniques for developing controllers for linear time-invariant systems, such as optimal and adaptive control are well established and could be used to control the nonlinear PMBDCM dynamics. For example, at this stage we could use LQR theory to design a feedback control law which minimizes some linear quadratic performance measure, or we could use model reference adaptive control techniques to design a controller such that the system states tract a desire trajectory. However, in order to physically implement these designs we must relate the control variables back to the original coordinate system. A more logical candidate for the feedback control design methodology is pole-placement, hence, the usual practice is to set the poles of the new linear system to satisfy some transient specification such as settling time (i.e., the time required to drive the trajectory of the system to some small neighborhood of the origin). Such a specification is appealing since we are guaranteed that the linear and nonlinear systems are related via a one-to-one mapping in the neighborhood of the origin. The poles of a linear controllable system in Brunovsky canonical form (11), are located at the origin. Therefore, relocating the poles is necessary to achieve stability. This stability can be achieved by placing the poles at an arbitrary point in the left-hand plane by state feedback and setting proper feedback gains. The feedback control laws are transformed back to the nonlinear space by inverse transformation (21). These control laws are

$$u_1 = \frac{y_4 - D(x)}{(1 + \frac{k_1}{k_2} x_4)} - \frac{k_1(G(x) - E(x))}{k_2 + k_1 x_4} \qquad (22)$$

$$u_2 = G(x) - E(x) \qquad (23)$$

where

$$G(x) = -c_1 y_1(x) - c_2 y_2(x) - c_3 y_3(x) - c_4 y_4(x)$$

and c_1, c_2, c_3, and c_4 are feedback gains.

5. Simulation Results

The exact linearization control laws were applied to the LPMBDCM plant, using a computer simulation of the model. The integration routine used was a fourth-order, fixed-increment Runge-Kutta integration method. The overall system diagram is shown in Figure 2. The translator position and two phase current signals are fed back to the controller for the generation of the exact linearization control laws. An initial error of 0.025 meter is selected for the nonlinear system, consequently, the initial states for linear system become

$$y(0) = [\,-.0065 \quad 0 \quad 0 \quad 0.318\,].$$

The feedback gains are

$$c_1 = 14640,\ c_2 = 5324,\ c_3 = 726,\ c_4 = 44.$$

The closed-loop poles of the linear system (11) with the above gains have negative real parts. They have been selected such that the system settles to 2% of the desired position, within 3.5 seconds,

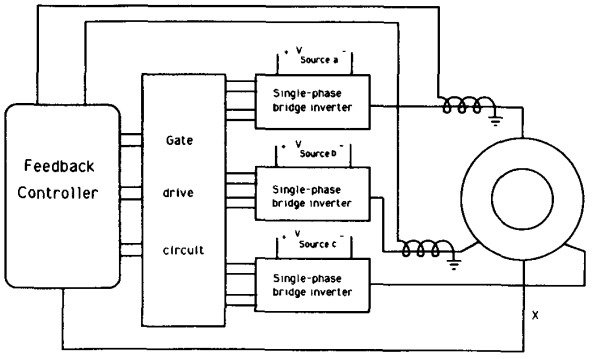

Figure 2: The overall system block diagram

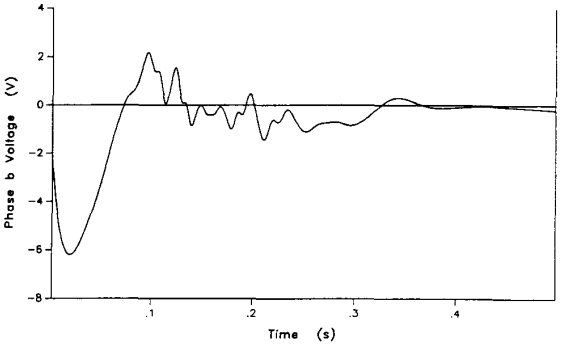

Figure 3: Phase "b" voltage vs. time

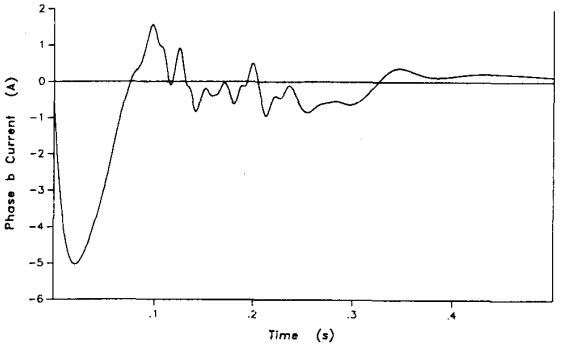

Figure 4: Phase "b" current vs. time

with no overshoot. Figures 3 and 4 show the input voltage and current, respectively, obtained from the closed loop simulation to the motor's "b" winding. Note these voltage and current signals contain high order harmonics in the range of 50-60 Hz. The high order harmonics present in the voltage and current signals are a direct consequence of the reluctance force. Verification of this claim was made by removing the reluctance force description from the model and observing that the high order harmonic components vanish as illustrated in Figure 5. Figures 6 and 7 show translator position and speed, respectively, obtained through the closed loop computer simulation. Notice that the simulated position and speed curves are smooth with no ripple.

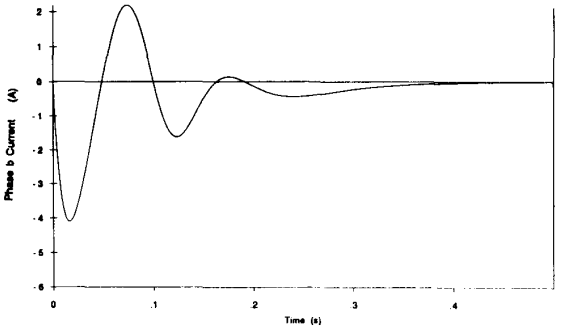

Figure 5: Phase "b" current vs. time with reluctance force removed

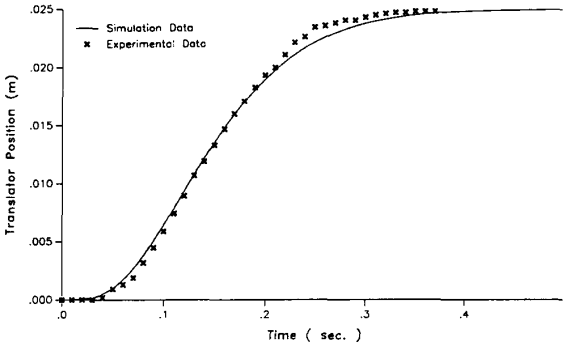

Figure 6: Translator position vs. time

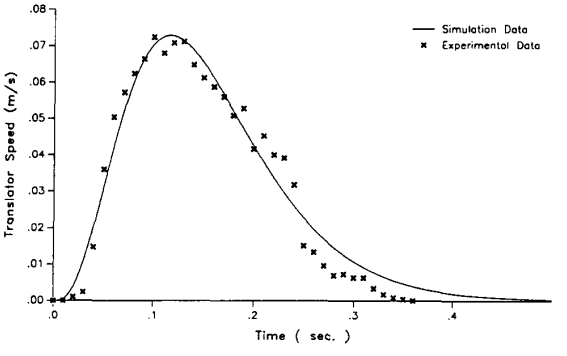

Figure 7: Translator speed vs. time

6. Experimental Results

Since the exact linearization control laws are in terms of the machine parameters, verification of the system model is necessary. Su has shown that the process of stabilizing a transformable nonlinear system by stabilizing its corresponding linear system is robust, if the mathematical model is a good representation of actual plant [14]. To verify this, we conducted a series of tests under dynamic conditions on the actual system and simulated the model under the same conditions for comparison. The dynamic tests were conducted by driving the motor with a full-bridge PWM inverter, controlled by a common two phase feeding scheme. Traces of position and phase current of the system were recorded simultaneously under 60 percent of input command and one pound load force. The experimental results of position and phase "a"

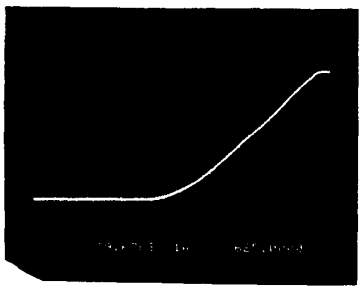

Vertical 14.5 mm/division
Horizontal 39.67 mSec./division

Figure 8: Photograph of translator position vs. time (two phase feeding control)

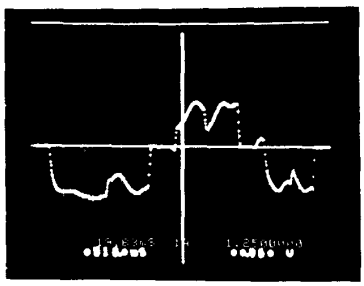

Vertical 1.33 A/division
Horizontal 25.5 mSec./division

Figure 9: Photograph of phase "a" current vs. time (two phase feeding control)

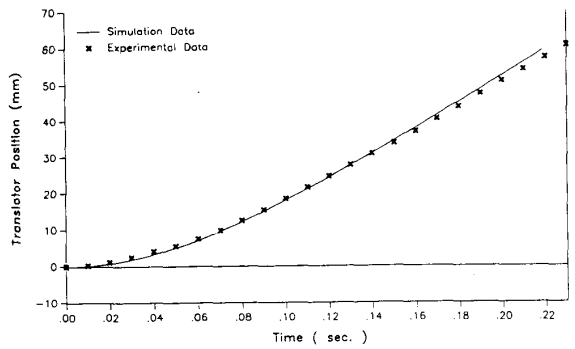

Figure 10: Translator position vs. time (two phase feeding control)

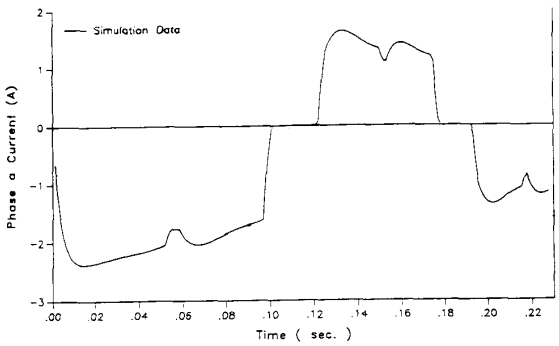

Figure 11: Phase "a" current vs. time (two phase feeding control)

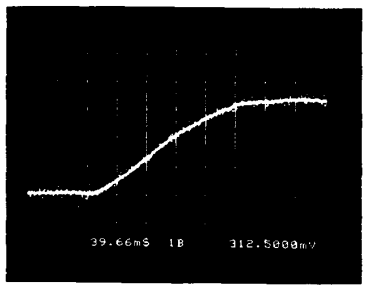

Vertical 7.37 mm/division
Horizontal 39.67 mSec./division

Figure 12: Photograph of translator position vs. time (open loop)

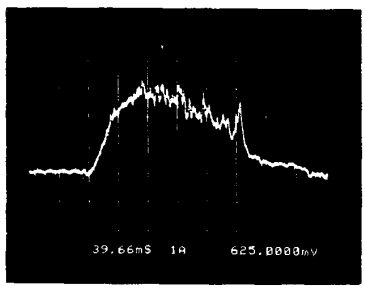

Vertical 25 mm/Sec./division
Horizontal 39.66 mSec./division

Figure 13: Photograph of translator speed vs. time (open loop)

current are illustrated in Figures 8 and 9, respectively, as photographs of the actual signals. The software simulation of the model under the same conditions of experimental setup are presented in Figures 10 and 11 for position and phase "a" current, respectively. The characteristics and the magnitude of the simulation and experiment results correlate reasonably well.

In an actual experimental set up each term of equations (22) and (23) must be generated, v_d and v_q must be calculated, and then transformed to obtain phase voltages in real time. This complex procedure involves approximately 184 floating point and 21 trigonometric operations which are now being developed using digital signal processing chips. This real time feedback implementation is necessary to remove cogging disturbances and to provide a fast accurate positioning over existing controls. However, in order to illustrate the validity of the exact linearization control laws, an open-loop experiment is conducted. For this test, the phase voltages of the computer simulation outputs are obtained and stored in the ROM of the microprocessor based PWM for a displacement of 0.025 meters. These voltages are then fed to the motor with no feedback signal present. Figure 12 shows the experimental position obtained by applying simulated voltages, under an open loop condition. Figure 13 shows the photograph of the speed signal under open loop condition. Also shown in Figures 6 and 7 are the simulated values of position and speed, respectively, with experimental data superimposed on the simulation results. Since these test have been conducted under open loop operation, they are expected to be rugged. The closed agreement suggests that the nonlinear plant model adequately represents the actual motor and that the linearization technique through which control was developed performed correctly. The validity of the control laws is apparent.

7. Conclusions

This paper has presented a nonlinear feedback control design methodology for a linear, permanent magnet brushless dc motor (LPMBDCM). A nonlinear state variable model for the motor was obtained and is subsequently transformed into a controllable linear model. Feedback control design was conducted for the linear model using pole placement techniques. The resulting control laws were then related back to the original coordinates. Also, simulation results of the control variables were injected into the actual nonlinear system in an experimental open loop setup. This control methodology systematically transforms the nonlinear system into a linear system allowing utilization of linear design theory and yielding smooth and ripple free operation under constant load conditions. The author notes that although the control objective cited in this paper is the position control of a LPMBDCM, this methodology can be readily applied to the control of rotary permanent magnet brushless dc motors. Currently, a PMBDCM with DSP-based controller is being developed and its performance will be the subject of a future paper.

APPENDIX A

The Linear Brushless dc Motor Parameters

L_d	6.845 mH
L_q	3.85 mH
r	1.2 Ω
λ_{max}	0.058 mWb
M	2.09 kg
Power	1/7 hp
Connection	series wye

APPENDIX B

Derivation of the State Variable Model

The general voltage equation of an electric machine in matrix form is

$$\overline{v}_{abcs} = \overline{r}_s \ \overline{i}_{abcs} + p\,(\overline{\lambda}_{abcs}) \qquad \text{(B1)}$$

where $\overline{v}_{abcs}$, $\overline{i}_{abcs}$, $\overline{\lambda}_{abcs}$ are vectors of phase voltages, currents, and flux linkages, respectively, and

$$\overline{r}_s = \begin{bmatrix} r & 0 & 0 \\ 0 & r & 0 \\ 0 & 0 & r \end{bmatrix}, \quad p(\cdot) = \frac{d(\cdot)}{dt},$$

and the flux linkages are

$$\overline{\lambda}_{abcs} = \overline{L}_s \ \overline{i}_{abcs} + \overline{\lambda}_m \qquad \text{(B2)}$$

where

$$\overline{L}_s = \begin{bmatrix} L_{ls}+L_A-L_B\cos(\frac{2\pi x_p}{\tau}) & -\frac{1}{2}L_A-L_B\cos2(\frac{\pi x_p}{\tau}-\frac{\pi}{3}) & -\frac{1}{2}L_A-L_B\cos2(\frac{\pi x_p}{\tau}+\frac{\pi}{3}) \\ -\frac{1}{2}L_A-L_B\cos2(\frac{\pi x_p}{\tau}-\frac{\pi}{3}) & L_{ls}+L_A-L_B\cos2(\frac{\pi x_p}{\tau}-\frac{2\pi}{3}) & -\frac{1}{2}L_A-L_B\cos2(\frac{\pi x_p}{\tau}+\pi) \\ -\frac{1}{2}L_A-L_B\cos2(\frac{\pi x_p}{\tau}+\frac{\pi}{3}) & -\frac{1}{2}L_A-L_B\cos2(\frac{\pi x_p}{\tau}+\pi) & L_{ls}+L_A-L_B\cos2(\frac{\pi x_p}{\tau}+\frac{2\pi}{3}) \end{bmatrix}$$

and (B3)

$$\overline{\lambda}_m = \lambda_{max}\begin{bmatrix} \sin(\frac{\pi x_p}{\tau}) \\ \sin(\frac{\pi x_p}{\tau}-\frac{2\pi}{3}) \\ \sin(\frac{\pi x_p}{\tau}+\frac{2\pi}{3}) \end{bmatrix}. \qquad \text{(B4)}$$

It is a well known practice to eliminate the position dependencies in system equations that are introduced through the inductance and flux linkage matrices. The selected process mathematically replaces the abc stator coils by fictitious qdo coils fixed to the translator. The following orthogonal transformation known as Park transformation can be applied

$$\overline{k} = \sqrt{\frac{2}{3}}\begin{bmatrix} \cos(\frac{\pi x_p}{\tau}) & \cos(\frac{\pi x_p}{\tau}-\frac{2\pi}{3}) & \cos(\frac{\pi x_p}{\tau}+\frac{2\pi}{3}) \\ \sin(\frac{\pi x_p}{\tau}) & \sin(\frac{\pi x_p}{\tau}-\frac{2\pi}{3}) & \sin(\frac{\pi x_p}{\tau}+\frac{2\pi}{3}) \\ \frac{1}{2} & \frac{1}{2} & \frac{1}{2} \end{bmatrix}. \qquad \text{(B5)}$$

A change of variables relation is introduced as

$$\overline{h}_{qdos} = \overline{k} \ \overline{h}_{abcs} \qquad \text{(B6)}$$

where

$$\overline{h}_{abcs} = [\,h_{as} \ \ h_{bs} \ \ h_{cs}\,]^T$$
$$\overline{h}_{qdos} = [\,h_{qs} \ \ h_{ds} \ \ h_{os}\,]^T$$

$\overline{h}$ can represent either voltage, current, or flux linkage. Since $\overline{k}$ has the property that $\overline{k}^{-1} = \overline{k}^T$ the transformed power is invariant.

Substituting (B6) and (B2) into (B1) and carrying out the matrix manipulation in expanded form leads to

$$v_q = r\,i_q + \frac{\pi}{\tau}\dot{x}_p\,L_d\,i_d + \sqrt{\frac{2}{3}}\,\frac{\pi}{\tau}\dot{x}_p\,\lambda_{max} + L_q\,p(i_q) \qquad \text{(B7)}$$

$$v_d = r\,i_d - \frac{\pi}{\tau}\dot{x}_p\,L_q\,i_q + L_d\,p(i_d) \qquad \text{(B8)}$$

$$v_o = r\,i_o + L_{ls}\,p(i_o). \qquad \text{(B9)}$$

where $L_d = L_{ls}+L_A+\frac{3}{2}L_B$, and $L_q = L_{ls}-L_A-\frac{3}{2}L_B$. For a balanced wye connected machine with floating neutral, $i_a+i_b+i_c=0$, hence, the zero sequence current is $i_o=\frac{1}{2}(i_a+i_b+i_c)=0$, and (B9) vanishes. Equations (B7) and (B8) are the same as equations (3) and (4).

For a magnetically linear field, and neglecting copper, hysteresis and eddy current losses, the electromagnetic force is

$$F(\overline{i}_{abcs}, x_p) = \frac{\partial w(\overline{i}_{abcs}, x_p)}{\partial x_p} \qquad \text{(B10)}$$

where

$$w(\overline{i}_{abcs}, x_p) = \left\{\frac{1}{2}\left[\overline{i}^{\,T}_{abcs}\left(\overline{L}_s - L_{ls}\overline{I}\right)\overline{i}_{abcs} + \overline{i}^{\,T}_{abcs}\,\overline{\lambda}_m\right]\right\} \qquad \text{(B11)}$$

and $\overline{I}$ is a 3x3 identity matrix. Substituting (B3), (B4), (B5), and (B6) into (B11) and performing the partial differentiation of (B10) and carrying out the matrix multiplication yields

$$F = \left(\frac{\pi}{\tau}\right)\left[(L_d-L_q)\,i_q i_d + \sqrt{\frac{2}{3}}\,i_q\,\lambda_{max}\right]. \qquad \text{(B12)}$$

Equation (B12) is the total developed force of the LPMBDCM, which is positive for motor action. The developed force is related to acceleration and speed by

$$F = M\frac{d\dot{x}_p}{dt} + \beta\,\dot{x}_p + F_L + F_R \qquad \text{(B13)}$$

where F_L, F_R are load and reluctance force, respectively. Equation (B13) is the same as (2).

APPENDIX C

Construction of Transformation

Before introducing the necessary and sufficient conditions for existence of a transformation, we will first introduce the following definitions from the differential geometry theory

Definition 1: For C^∞ vector fields f and g on $\mathbb{R}^n$, the Lie bracket of f and g is given by $[f,g] \triangleq \frac{\partial g}{\partial x}f - \frac{\partial f}{\partial x}g$ where $\frac{\partial g}{\partial x}f$ and $\frac{\partial f}{\partial x}g$ are Jacobian matrices.

Definition 2: A collection of C^∞ vector fields $\{f_1, f_2, \ldots, f_n\}$ on $\mathbb{R}^n$ is involutive if there exist C^∞ functions $\gamma_{ijk}(x)$ such that

$$[f_i, f_j] = \sum_{k=1}^{n} \gamma_{ijk}(x) f_k(x), \text{ for } 1 \le i, j \le n, i \ne j.$$

The following necessary and sufficient conditions from [13] (or [11]) must be satisfied for existence of a transformation.

Theorem 1: The system (9) is equivalent to the system (11), where the state variables x_1, x_2, x_3, x_4 lie in a sufficiently small open neighborhood V of the origin in $\mathbb{R}^4$, if and only if the following conditions hold on V:

i) The set $c = \{ g_1, [f,g_1], (ad^2f, g_1), g_2 \}$ has full rank.

ii) The set $c_1 = \{ g_1, [f,g_1], g_2, [f,g_2] \}$ is involutive.

iii) The span of c_1 is equal to the span of $c_1 \cap c$.

The results of the formulation of the set c are given in [9], and all three conditions of theorem 1 has been satisfied for **LPMBDCM**. We now introduce the following theorem from [13] which is employed to construct a non-unique transformation.

Theorem 2: If the system (9) is T-related to the system (11) on U, then

a) $\dfrac{\partial T_j}{\partial u_k} = 0$, $j = 1,2,3,4$ and $k = 1,2$,

b) the 2 x 2 matrix $\left[\dfrac{\partial T_j}{\partial u_k}\right]$, $j = 5,6$ and $k = 1,2$ is nonsingular on U,

c) the following partial differential equations hold on U

$$< dT_m, g_i > = 0, \quad m = 1,2, \quad \text{and} \quad i = 1,2, \tag{C1}$$

where $< dT_m, g_i > = \dfrac{\partial T_m}{\partial x_i} g_i$

and $$< dT_m, f > = T_{m+1}, \quad m = 1,2, \tag{C2}$$

$$< dT_3, f + \sum_{i=1}^{2} u_i g_i > = T_5 \tag{C3}$$

$$< dT_4, f + \sum_{i=1}^{2} u_i g_i > = T_6. \tag{C4}$$

To apply Theorem 2 to our system we will first expand (C1) and (C2) in the following manner:

$$< dT_1, g_1 > = < dT_1, g_2 > = < dT_2, g_1 > = < dT_2, g_2 > = 0$$

$$T_2 = < dT_1, f >, \; T_3 = < dT_2, f >. \tag{C5}$$

Application of Leibnitz's formula yields

$$< dT_1, (ad^0 f, g_1) > = 0 \tag{C6}$$

$$< dT_1, (ad^0 f, g_2) > = 0 \tag{C7}$$

$$< dT_1, (ad^1 f, g_1) > = 0 \tag{C8}$$

$$< dT_1, (ad^1 f, g_2) > = 0 \tag{C9}$$

$$< dT_4, (ad^0 f, g_1) > = 0 \tag{C10}$$

$$< dT_4, (ad^0 f, g_1) > = 0. \tag{C11}$$

where $(ad^0 f, g) = g$, and the successive Lie brackets defined as $(ad^k f, g) \triangleq [f, (ad^{k-1} f, g)]$.

Also from part c) of theorem 2, (C3), (C4), and Leibnitz formula we obtain

$$T_5 = (dT_3, f) + \sum_{i=1}^{2} (u_i < dT_1, (ad^2 f, g_i) >) \tag{C12}$$

$$T_6 = (dT_4, f) + \sum_{i=1}^{2} (u_i < dT_4, (ad^0 f, g_i) >) \tag{C13}$$

From condition b) of Theorem 2, the following 2 x 2 matrix should be nonsingular in order to solve for u_1 and u_2

$$\begin{bmatrix} < dT_1, (ad^2 f, g_1) > & < dT_1, (ad^2 f, g_2) > \\ < dT_4, (ad^0 f, g_1) > & < dT_4, (ad^0 f, g_2) > \end{bmatrix} \tag{C14}$$

Thus, in order to construct the necessary transformation for system (9), partial differential equations (C6)-(C11) and (C12)-(C13) must be solved with the condition that the matrix in (C14) remains nonsingular. It is a straightforward but lengthy task to show that the preceding construction procedure results in the following transformation:

$$s_1 = \frac{x_1}{k_2} \tag{C15}$$

$$s_2 = \frac{-x_2}{k_2} + (k_3 + k_4)\frac{x_1}{k_2} \tag{C16}$$

$$s_3 = x_3 - \frac{k_4}{k_2} x_2 + \left(\frac{k_4 k_3}{k_2} - k_6\right) x_1 \tag{C17}$$

$$s_4 = x_4 + \left[\sum_{i=1}^{4} k_{9i} \sin\omega_i + k_{10} \right] \frac{k_8}{k_2} x_1 \tag{C18}$$

where s_1, s_2, s_3, and s_4 are real parameters. Thus, (C15)-(C18) is a mapping from $\mathbb{R}^4$ to $\mathbb{R}^4$ that transforms

$$(s_1, s_2, s_3, s_4) \to ((x_1(s), x_2(s), x_3(s), x_4(s)) \tag{C19}$$

The noncharacteristic matrix of this transform evaluated at the origin is

$$\begin{bmatrix} \frac{\partial x_1}{\partial s_1} & \cdots & \frac{\partial x_1}{\partial s_4} \\ \vdots & & \vdots \\ \frac{\partial x_4}{\partial s_1} & \cdots & \frac{\partial x_4}{\partial s_4} \end{bmatrix} = \begin{bmatrix} k_2 & 0 & 0 & 0 \\ k_2(k_3+k_4) & -k_2 & 0 & 0 \\ k_2 k_6 + k_4^2 & -k_4 & 1 & 0 \\ 0 & 0 & 0 & 1 \end{bmatrix} \tag{C20}$$

We remark that the columns of right hand side of (C20) are $(ad^2 f, g_1)$, $(ad^1 f, g_1)$, g_1, and g_2, which are vector fields in C. Furthermore, (C20) has a nonzero determinant which implies that the mapping defined by (C19) is a diffeomorphism on an open neighborhood W of the origin in $\mathbb{R}^4$.

Now, let U be a sufficiently small open set about the origin in the image of W. Let us define our new linear state variables as y_1, y_2, y_3, and y_4. Let $y_1 = T_1 = s_1$ and note that

$$\frac{\partial T_1}{\partial s_i} = 0 \quad \text{for } i = 2,3,4 .$$

Rewriting (C5) yields

$$T_2 = \frac{\partial T_1}{\partial x} f = \begin{bmatrix} \frac{1}{k_2} & 0 & 0 & 0 \end{bmatrix} f = \frac{x_2}{k_2} = y_2 \tag{C21}$$

$$T_3 = \frac{\partial T_2}{\partial x} = \frac{k_3}{k_2} x_2 + \left(\frac{k_1}{k_2} x_4 + 1\right)(x_3 + x_{3d}) + \sum_{i=1}^{4} \frac{k_{9i}}{k_2} \sin\omega_i + \frac{k_{10}}{k_2} = y_3 \tag{C22}$$

$$T_4 = x_4 + \left[\sum_{i=1}^{4} k_{9i} \sin\omega_i + k_{10} \right] \frac{k_8}{k_2} x_1 = y_4 \tag{C23}$$

and, from earlier,

$$T_1 = \frac{x_1}{k_2} = y_1 . \tag{C24}$$

We are now ready to solve u_1 and u_2 by first showing the matrix defined by (C14) is nonsingular. Evaluating (C14) yields

$$\begin{bmatrix} < dT_1, (ad^2 f, g_1) > & < dT_1, (ad^2 f, g_2) > \\ < dT_4, (ad^0 f, g_1) > & < dT_4, (ad^0 f, g_2) > \end{bmatrix} = \begin{bmatrix} 1 & \frac{k_1}{k_2} x_{3d} \\ 0 & 1 \end{bmatrix}$$

which clearly has a nonzero determinant.

Upon verifying that the matrix in (C14) is nonsingular, we are ready to find the transformed control variables. From (C3) we can write

$$T_5 = \frac{\partial T_3}{\partial x}(f + u_1 g_1 + u_2 g_2)$$

Evaluating $\dfrac{\partial T_3}{\partial x}$, we obtain

$$\frac{\partial T_3}{\partial x} = \left[\sum_{i=1}^{4} \frac{6\pi i k_{9i}}{\tau k_2} \cos\omega_i \quad \frac{k_3}{k_2} \quad \frac{k_1}{k_2} x_4 + 1 \quad \frac{k_1}{k_2}(x_3 + x_{3d}) \right]$$

therefore,

$$T_5 = D(x) + \left(1 + \frac{k_1}{k_2} x_4\right) u_1 + \frac{k_1}{k_2}\left(x_3 + x_{3d}\right) u_2 \equiv v_1 \qquad \text{(C25)}$$

where

$$D(x) = \sum_{i=1}^{4} \frac{6\pi i k_{9i}}{\tau k_2} \cos\omega_i x_2 + \frac{k_3^2}{k_2} x_2 + \frac{k_1 k_3}{k_2} x_3 x_4 + k_3\left(x_3 + x_{3d}\right) + \frac{k_3}{k_2} x_4 + k_1 x_{3d} + \frac{k_3 k_9}{k_2} \sin\omega - \frac{k_3 k_{10}}{k_2} + (k_4 x_3 + k_5 x_2 x_4 + k_6 x_2)\left(\frac{k_1}{k_2} x_4 + 1\right) + \frac{k_1}{k_2}\left(x_3 + x_{3d}\right)(k_7 x_4 + k_8 x_2 x_3 + k_8 x_2 x_{3d})$$

Similarly, (C4) can be written as

$$T_6 = \frac{\partial T_4}{\partial x}\left(f + u_1 g_1 + u_2 g_2\right)$$

Evaluating the above equation produces

$$T_6 = E(x) + u_2 \equiv v_2 \qquad \text{(C26)}$$

where

$$E(x) = k_7 x_4 + k_8 x_2 x_3$$

Since (C13) is nonsingular for our system, we can solve for u_1 and u_2 from the inverse function theorem. Writing (C25) and (C26) in matrix form we obtain

$$\begin{bmatrix} v_1 \\ v_2 \end{bmatrix} = \begin{bmatrix} 1 + \frac{k_1}{k_2} x_4 & \frac{k_1}{k_2}(x_3 + x_{3d}) \\ 0 & 1 \end{bmatrix} \begin{bmatrix} u_1 \\ u_2 \end{bmatrix} + \begin{bmatrix} D(x) \\ E(x) \end{bmatrix}$$

and therefore,

$$\begin{bmatrix} u_1 \\ u_2 \end{bmatrix} = \begin{bmatrix} \left(1 + \frac{k_1}{k_2} x_4\right)^{-1} & \frac{-k_1(x_3 + x_{3d})}{k_2 + k_1 x_4} \\ 0 & 1 \end{bmatrix} + \begin{bmatrix} v_1 - D(x) \\ v_2 - E(x) \end{bmatrix} \qquad \text{(C27)}$$

ACKNOWLEDGEMENT

The author wishes to thank Dr. J. J. Cathey for his support on constructing the motor and B. Walcott for several helpful discussions.

REFERENCES

[1] T. J. E. Miller, *Brushless Permanent-Magnet and Reluctance Motor Drives*, Clarendon Press, Oxford, 1989.

[2] N. A. Demerdash and T. W. Nehl, "Dynamic Modeling of Brushless DC Motors for Aerospace Actuation," *IEEE Transactions on Aerospace and Electronic systems*, Vol. AES-16, pp. 811-821, November 1980.

[3] P. C. Krause, R.R. Nuccra, R. J. Krefta, and O. Wasynczuk, "Analysis of a Permanent Magnet Synchronous Machine Supplied from a 180° Inverter with Phase Control," *IEEE Transactions on Energy Conversion*, Vol. EC-2, No. 3, pp. 423-431, September 1987.

[4] Meshkat and Persson, "Optimum Current Vector Control of a Brushless Servo Amplifier using Microprocessors," *IEEE-IAS Annual Meeting*, pp. 451-457, Oct. 1984.

[5] Le-Huy, Perret, and Fuillet, "Minimization of Torque Ripple in BDCM Drives," *IEEE-IAS Transactions*, Vol. IA-22, No. 4, pp. 748-755, 1986.

[6] H. Hashimoto, H. Yamamoto, S. Yanagisawa, and F. Harashima, "Brushless Servo Motor Control using Variable Structure Approach," *IEEE-IAS Transactions*, Vol. 24, No. 1, pp. 160-170, 1988.

[7] M. A. El-Sharkawi, "Development and Implementation of High Performance Variable Structure Tracking Control for Brushless Motors," *IEEE Transactions on Energy Conversion*, Vol. 6, No. 1, pp. 114-119, March 1991.

[8] N. Hemati, J. S. Thorp, and M. C. Leu, "Robust Nonlinear Control of Brushless dc Motors for Direct-Drive Robotic Applications," *IEEE Transactions on Industrial Electronics*, Vol. 37, No. 6, pp. 460-468, 1990.

[9] P. Famouri, "Exact Linearization of a Linear PM Brushless dc," *Ph.D. dissertation*, University of Kentucky, 1989.

[10] R.W. Brockett, "Feedback Invariants for Nonlinear Systems," *IFAC Congress*, 1978.

[11] B. Jakubczky, W. Respondek, "On Linearization of Control Systems," *Bulletin de L'academie polonasise des science*, series des sciences mathematiques Vol.XXVIII, No. 9-10, pp. 517-522, 1980.

[12] R. Su, "On the Linear Equivalents of Nonlinear Systems," *Systems and Control Letters*, Vol. 2, pp. 48-52, 1982.

[13] L. Hunt, R. Su, and G. Meyer, "Design for Multi-Input Nonlinear Systems," *Differential Geometric Control Theory*. Burkhauser, pp. 268-298, 1983.

[14] R. Su, G. Meyer, and L. Hunt, "Robustness in Nonlinear Control," *Differential Geometric Control Theory*. Burkhauser, pp. 316-337, 1983.

Parviz Famouri received the B.S. degree in applied mathematics from Kentucky State University in 1981. He then began his studies at the University of Kentucky, where he received the B.S.E.E., M.S.E.E., and Ph.D. degrees in 1982, 1986, and 1990, respectively. Since 1990, he has been at West Virginia University, where he is an assistant professor of Electrical Engineering.

His research interests are in the control of electric machines and power electronics.